Lab Report A-IV

Emma Modesitt, Megan Pramojaney, and Nathan McCarley
Department of Physics and Astronomy, The University of North Carolina at Chapel Hill
(Physics 281, Group α)
(Dated: August 15, 2023)

Compton scattering of x-ray photons provides evidence that photons possess particle-like behavior, a property which can be used to determine Planck's constant. We measured the rates at which x-ray photons scattered off of an aluminum block both with and without passing through a copper filter, then plotted the relationship of said rates to the wavelength of the scattered photons. From this, we found Planck's constant to be $(9 \pm 3) \times 10^{-34}$ J $\cdot$ s. The accepted value of Planck's constant does fall in the range of our uncertainty but we did have a wide range of uncertainty, implying there were some issues with precision in our experimental measurements.

I. INTRODUCTION

Though classical physics predicted that scattered photons should have exactly the same wavelength as inbound light, several experiments in the early 20th century demonstrated that scattered wavelength was greater than incident wavelength, indicating a loss of energy due to the scattering process [1]. Such behavior was not explainable until Arthur Compton's paper was published in 1923, in which he argued that photons, although massless, still possessed momentum and therefore obeyed the same momentum and energy conservation laws as particles. He then verified this theory by observing the wavelength shifts of x-rays from a molybdenum source scattered by a graphite target [1]. This served as one of the first ways to study the particle-like properties associated with light. We aim to recreate Compton's experiment, this time with an aluminum target, in order to determine Planck's constant.

II. THEORETICAL BACKGROUND

A. X-Ray Scattering

In the first part of our experiment, we looked at the scattering of x-ray photons when they were diffracted by a NaCl crystal. The x-ray apparatus with the goniometer and Geiger counter can measure then angle between the crystal and the collimator. Using the relation

$$n\lambda = 2d \sin\theta, \tag{1}$$

we can see how the diffraction angle, θ, and wavelength, λ, of the scattered x-rays are related. Once an electric potential U is applied between the anode and cathode of the apparatus, high energy x-ray photons are directed through the collimator and enter the chamber where they are interact with the crystal and scatter x-ray photons, which are then detected by the Geiger counter. The rate at which the x-rays are detected, R_{NaCl0}, at each diffraction angle, is a dependent variable in our experiment. We will place a copper foil filter over the Geiger counter and record the counts/s of x-rays that are detected, R_{NaCl1}. The ratio of these values at a range of diffraction angles

$$T_{Cu} = \frac{R_{NaCl_0}}{R_{NaCl_1}}, \tag{2}$$

compared to data without the filter gives us T_{Cu}, the transmission coefficient of the copper filter. This can be plotted as a function of wavelength derived from Equation 1. Once the non-linear relationship between T_{Cu} and λ is defined, we can measure the input wavelength, λ_1 and output wavelength, λ_2, when an aluminum block is used instead of the NaCl crystal. This is done by measuring the count rate of x-ray photon counts without the filter (R_0), with the filter placed on the collimator (R_1) and with the filter placed on the Geiger counter (R_2). The resulting transmission coefficients,

$$\frac{R_1}{R_0} = T_{Cu}(\lambda_1) \tag{3}$$

and

$$\frac{R_2}{R_0} = T_{Cu}(\lambda_2) \tag{4}$$

correspond to when the filter placed on the collimator and when the filter placed on the sensor respectively, with both transmission coefficients being a function of their respective wavelengths.

B. Compton Scattering

Compton scattering occurs when a high-energy photon collides with a bound electron and following the conservation of energy and momentum, a photon with a longer wavelength is scattered. In this experiment, an aluminum block will be our method to scatter photons. Similar to the NaCl crystal, high energy x-ray photons will be directed towards the block. Following Compton's discovery that momentum and energy are conserved during the collision, we see that

$$p_1 = p_2 + p_e \tag{5}$$

and

$$E_1 + E_{e_i} = E_2 + E_{e_f}, \tag{6}$$

where p_1 and E_1 correspond to the initial x-ray photon exiting the collimator, p_2 and E_2 correspond to the photon that is scattered from the block, and p_e, E_{e_i}, and E_{e_f} correspond to the electron that is hit during the collision from the original photon. Figure 1 depicts how the original photon with λ_1 collides with the bound electron within the block and then a photon with a longer wavelength λ_2 leaves the collision[1]. The electron has energy

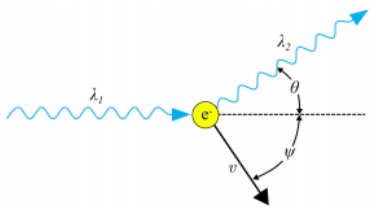

FIG. 1: The collision above begins with an x-ray photon with a wavelength λ_1 colliding with an electron within the aluminum block. After the collision, a lower energy x-ray photon with a wavelength λ_2 radiates out at a certain angle θ. The electron also recoils at a different angle and velocity.

both before and after the collision, but only possesses momentum when it starts moving after the collision. Recalling that $E = pc$ and

$$p = \frac{hf}{c} \tag{7}$$

where f is the frequency of the photon, we can write Equation 6 as

$$hf_1 + m_e c^2 = hf_2 + \sqrt{p_e^2 c^2 + m_e c^4} \tag{8}$$

where h is Planck's constant, m_e is the mass of an electron, and c is the speed of light. The momentum of the photons can be described as

$$p_1 = \frac{E_1}{c} = \frac{h}{\lambda_1} \text{ and } p_2 = \frac{E_2}{c} = \frac{h}{\lambda_2}. \tag{9}$$

Using the scalar product rule-in order to find the square of the magnitude of p_e- on Equation 5, we find that

$$(p_e c)^2 = (p_1 - p_2)(p_1 - p_2) = p_1^2 + p_2^2 - 2p_1 p_2 \cos\theta, \tag{10}$$

and the angle θ represents the angle between incident photon and exiting photon. We can then substitute Equation 9 into Equation 10 and multiply by c^2, ending up with

$$(p_e c)^2 = (hf_1)^2 + (hf_2)^2 - 2h^2 f_1 f_2 \cos\theta. \tag{11}$$

Since both the conservation of energy and momentum equations now have a factor of $(p_e c)^2$, we can set Equation 11 and Equation 8 equal to each other. We simplify by squaring Equation 8 and then eliminating the $h^2 f_1^2 + h^2 f_2^2$ factors from both Equation 11 and Equation 8. We further simplify this equation into

$$\frac{1}{m_e c^2}(1 - \cos\theta) = \frac{1}{hf_2} - \frac{1}{hf_1}. \tag{12}$$

We know that a photon's frequency can be found using $c = \lambda f$, so Equation 12 turns into

$$\frac{h}{m_e c}(1 - \cos\theta) = \lambda_2 - \lambda_1 \tag{13}$$

which can then be plotted linearly.

III. METHODS

A Leybold 554 800 x-ray apparatus with molybdenum anode and goniometer-mounted Geiger counter was used to conduct the experiment (Figure 2). A PC connected to the x-ray apparatus via USB was used to run the software controlling the x-ray apparatus's settings.

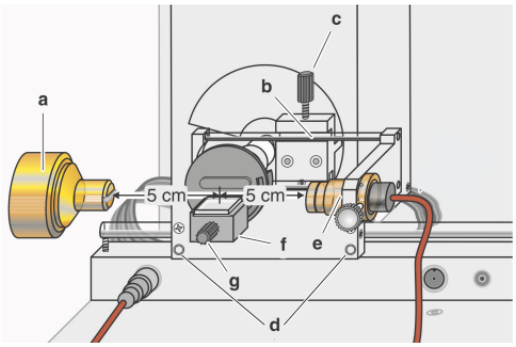

FIG. 2: Diagram of goniometer inside the main chamber of the Leybold apparatus. The NaCl crystal target is mounted in the sample holder, **f** using knob **g**. The distance between the collimator, **a** and the target is adjusted using knob **d**. The distance between the target and the sensor, **e**, is adjusted using knob **c** and sliding the goniometer arm **b** in and out.

To determine the transmission coefficient of x-rays through copper foil as a function of wavelength, we first removed any filters on the goniometer. The goniometer and sensor were initialized to the home position and mounted the NaCl cyrstal into the target holder. Then, the distance between the target and the sensor was set to 5 cm and the distance between the target and the collimator was set to 5 cm. A scan from 0° to 8° in increments of 0.2° was run, with the scan interval set to $\Delta t = 1$ s, the tube voltage set to $U = 30$ kV, and the current set to $I = 1.00$ mA. We kept our angle small so we did not need to account for higher order Bragg diffraction, which began at 8.42°.

Finding this range of angles to provide a suitable region for determining the aforementioned transmission coefficient, we repeated the above process with 1 pm resolution. Then, we inserted the copper filter into the goniometer and repeated the process a final time with the

increased resolution. We used these two data sets to plot T_{Cu} as a function of wavelength and chose to apply an exponential fit. This was done because our data set followed an exponential curve, and later calculations depended on our trend line function. Thus, an accurate trend line function was necessary to obtain accurate calculations later on.

To measure Compton scattering, we replaced the NaCl crystal with the aluminum block. We then set the distance between the collimator and the target to 7.4 cm and the distance between the target and the Geiger counter to 4 cm. The target and sensor were set to rotate independently and the target angle was set to 20°. The tube voltage and current remained the same.

The resulting count rate at each angular step was collected with no copper filter (R_0), with the copper filter mounted on the collimator (R_1) and with the copper filter mounted on the Geiger counter (R_2). The data without the copper filter was collected at a precision of 5° with a time interval of 60 s. The data without the copper filter was collected at a precision of 5° with the scan interval set to $\Delta t = 60$ s. Both data sets collected with the copper filter were collected at a precision of 5° with the scan interval set to $\Delta t = 120$ s. Equation 3 and 4 were then used to find λ_1 and λ_2 for each angle θ. A linear fit was then made in accordance to Equation 13 to find the experimental value for Plank's constant. Uncertainty in this value originates from uncertainty in the transmission dependence function, and was propagated through quadrature.

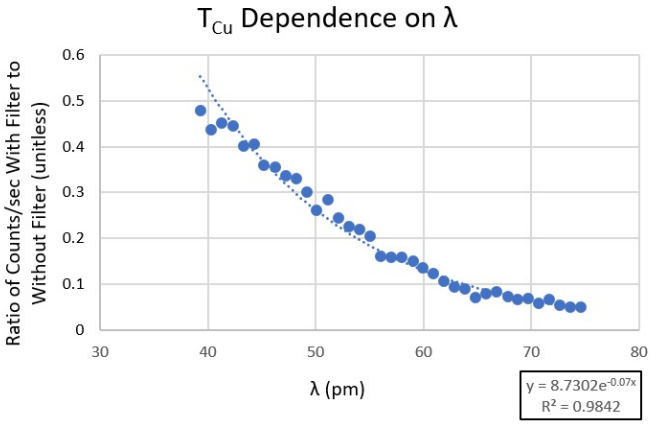

FIG. 3: The relationship between Transmission rate and wavelength.

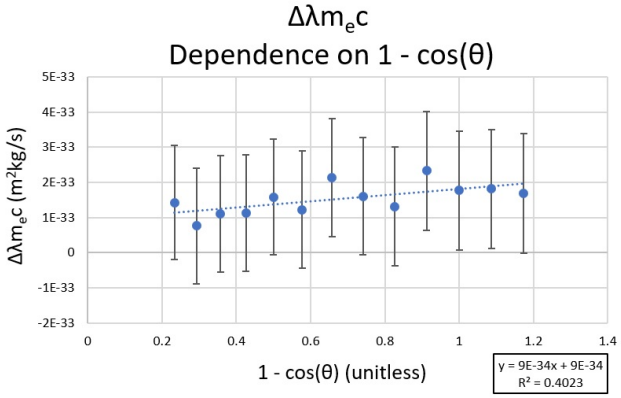

FIG. 4: The slope of the linear fit is equal to Planck's constant, h.

IV. RESULTS

For the trials conducted with the NaCl crystal, T_{Cu} was graphed as a function of λ in order to fit an exponential function to $T_{Cu}(\lambda)$. Fig. 3 depicts this graph. Using Excel, $T_{Cu}(\lambda)$ was found to be

$$T_{Cu}(\lambda) = (8 \pm 1)e^{(-0.070 \pm 0.002)\lambda}, \tag{14}$$

with the uncertainty in the slope and y-intercept of the fit being given by Excel's LINEST function.

Using the derivations in the Theoretical Background, we obtained two wavelengths, λ_1 and λ_2, from Equations 3 and 4. The difference $\Delta\lambda$ in these wavelengths was then calculated for each angle measurement in the second part of the experiment. Plotting $\Delta\lambda m_e c$ against $(1 - cos\theta)$ produced a linear fit with a slope of h. This is shown in Figure 4.

Using LINEST, we found the value of the slope (h) to be $(9 \pm 3) \times 10^{-34}$. The error bars were found by propagating the uncertainty in the components of Figure 4's y-values through quadrature.

V. DISCUSSION AND CONCLUSIONS

The accepted value of Planck's constant h is 6.63×10^{-34}, and our calculated value was $(9 \pm 3) \times 10^{-34}$. Though the uncertainty is relatively large, the literature value of h falls within the bounds of our calculations. Uncertainty in some of the measured values was either hard or impossible to determine. The Leybold apparatus did not have a listed uncertainty for *counts/sec*. Further, because of its precision, there was not an uncertainty for the angle measurements, or for the wavelengths from the first part of the experiment. Error mainly comes from the fact that *counts/sec* was so low for the second part that the "bucket size", or interval of measurement, needed to be high in order to gather enough data to calculate an accurate average. However, this blurs the lines between measurements, as the average includes values that are far from the designated "bucket location" — the angle for which *counts/sec* is measured.

VI. ACKNOWLEDGMENTS

The experiment was performed by E.M. and N.M., and M.P. recorded the data. E.M. wrote the Abstract and Theoretical Background sections. M.P. wrote the Introduction and Methods section. N.M. wrote the Results and Discussion and Conclusions section. Clarifying questions were answered by Ben Levy.

[1] Lab A-IV Manual
https://sakai.unc.edu/access/content/group/41081125-b301-4ad9-8173-970601749ad6/Lab\%20Manuals/Lab\%20A-IV\%3A\%20Compton\%20Scattering/Lab\%20A-IV\%20Compton\%20Scattering.pdf